Kinetics of the martensitic transition in In-Tl alloys

H. Abe, M. Ishibashi, K. Ohshima, and T. Suzuki
Institute of Applied Physics, University of Tsukuba, Tsukuba 305, Japan

M. Wuttig
Department of Materials and Nuclear Engineering, University of Maryland, College Park, Maryland 20742-2115

K. Kakurai
Institute for Solid State Physics, University of Tokyo, Roppongi, Minatoku, Tokyo 106, Japan
(Received 25 April 1994)

The kinetics of the martensitic transition in In-Tl alloys has been studied by x-ray- and neutron-diffraction methods. A characteristic waiting time appears at fixed temperature above M_s, the normal martensitic phase transition start temperature. A similar waiting time is also seen for inverse phase transitions. A peculiar temperature T_p, which is above M_s, but below T_0, is found to exist. The time development of x-ray-diffraction patterns shows a very different behavior whether the temperature is above T_p or below T_p. It is found that ideal nucleation and growth take place between T_p and T_0. Between T_p and M_s, the kinetics of the phase transition is more complicated. In order to understand the kinetics of the phase transition, the temperature-dependent waiting time curve in In-Tl alloys is calculated using the Roitburd method [A. L. Roitburd, Mater. Sci. Eng. **A127**, 229 (1990)] and is found to be in good agreement with experimental results.

I. INTRODUCTION

The nonequilibrium kinetics of the nucleation and growth in martensitic transitions has recently been drawing attention. In particular, athermal and isothermal martensitic transitions have been investigated from the thermodynamical point of view on nucleation. The amount of athermal martensite has been considered to be a function of temperature only. The isothermal martensite transition has been considered not to take place until the temperature is brought down below M_s, the martensitic transition start temperature, which is always below the thermodynamical equilibrium temperature, T_0, between the parent and low-temperature phases. On the other hand, the amount of isothermal martensite has been thought to be dependent on both temperature and time, where a waiting time or an incubation time is needed until the martensite transition starts while the temperature is kept constant. The incubation time in the first-order phase transition other than martensitic transition has been studied for the ordering process during order-disorder transitions in Cu_3Au (Refs. 1–3) and the phase transition from the NaCl to the CsCl structure in alkali halides at high pressure.[4]

Although the kinetics of the martensitic transition has been studied theoretically and experimentally, many problems still remain unclear. Because the reaction path for the martensitic transition has not yet been established, the theoretical studies have often been carried out using a classical or semiclassical approach for the nucleation[5–7] without verifying experimental results. Experimental studies of the kinetics of the martensitic transition have been difficult because of their quickness. Roitburd[8] estimated the nucleation barrier by introducing multiple-domain (twinned) martensite and single-domain martensite; the nucleation barrier for multiple-domain martensite is 10^3 times less than single martensite above M_s. On the other hand, Kakeshita *et al.*[9] have performed the systematic study of the incubation time in Fe-Ni-Mn alloys under magnetic field or hydrostatic pressure. They have interpreted their experimental results by introducing the cluster model. This model is based on the probability related to the nucleation barrier. Moreover, it is predicted that the athermal martensitic transition can be explained in the same kinetics as the isothermal martensitic transition.[10]

The martensitic transition in metallic sodium is one of typical athermal ones. Although the difference between M_s and A_s (reverse transition start temperature) in In-Tl alloys is less than 5 K, the martensitic transition has been considered to be athermal. The presence of the incubation time in these martensites has never been seen previously,[11,12] due to narrow temperature range and long incubation times above M_s. However, an accurate temperature controller made it possible to measure diffraction patterns at every 0.5 K step with an accuracy of 0.1 K. At the temperature above M_s but below T_0, we have found that it took a long time to start to transform into the low-temperature phase, i.e., the integrated intensity of the low-temperature phase started to gradually increase. Therefore, more detailed x-ray and neutron experiments have been performed to study the relationship between the nucleation barrier and the incubation time from a microscopic point of view.

In-Tl alloys were selected to study the above topics in this experiment, since they have an ideal disordered state in which no short-range order diffuse intensity was measured. In addition, the crystalline state at room tempera-

ture can completely recover that of the parent phase after inverse transition in spite of the first-order phase transition. Hence, many experiments can be repeated using the same sample. On the other hand, many studies of In-Tl alloys have been investigated from the viewpoint of the precursor phenomena or the soft-phonon mode as a weak second-order phase transition. No soft-phonon mode was found in various branches by the latest neutron study.[13] Hence, the soft-phonon model is not adequate to understand the nucleation process of the martensite.[14] Furthermore, the recent x-ray diffuse scattering study[12] has confirmed the absence of the precursor phenomena. This means that the nucleation problem in In-Tl alloys should be treated as a typical first-order phase transition, not as a near second-order phase transition.

II. EXPERIMENT

A single crystal of In-23 at. % Tl alloy, prepared at the University of Maryland, was used both in the x-ray- and neutron-diffraction experiments. The crystal was a cube of $5\times5\times5$ mm^3. Its face was cut parallel to (110) plane and etched chemically in a solution of 50-ml HNO_3 and 50-ml-distilled water. The mosaic spread of this specimen was about 2.1 min.

First, we performed an x-ray-diffraction experiment on a four-axis diffractometer where MO $K\alpha$ was used as the primary beam. A highly oriented pyrolytic graphite (HOPG) (002) crystal was used to obtain a monochromated beam. High-resolution x-ray experiment was needed to resolve the time change of the closely spaced three peaks at constant temperature; two of them are the $(202)_{fct}$ Bragg reflections from variant I and variant II of the low-temperature phase and the other is the $(220)_{fcc}$ Bragg reflection from the parent phase. Second, the x-ray of the wave length of 0.070 926 nm (Mo $K\alpha_1$) monochromated by Si(311) was used. The incident beam divergency in Si(311) was about 2.0 min, which is ten times narrower than that in HOPG (002).

The cryostat was a closed-cycle cryogenic refrigerator manufactured by Air Products Co. (Model DE201) and mounted on a Huber Eulerian cradle (Model 511.1). The temperature of the sample was controlled with an accuracy of 0.1 K.

The neutron-diffraction measurements were performed at the beam line 5G of JRR-3M reactor, Japan Atomic Energy Research Institute, Tokai, Japan. Pyrolytic graphite (PG) was used both as a monochromator and analyzer, while PG in front of the monochromator was used as a filter to discriminate the $\lambda/2$ component. The collimations before the monochromator and after the sample and after the analyzer were 40'-40'-40'-40' and the incident wavelength was 0.235 nm. The triple-axis spectrometer of Institute for Solid State Physics, University of Tokyo, was equipped with the same type cryostat as the x-ray apparatus. The temperature of the sample was also stabilized within 0.1 K.

III. RESULTS AND ANALYSIS

The specimen was annealed for 12 h at room temperature before starting each measurement. After that, the full width at half maximum (FWHM) of $(220)_{fcc}$ Bragg reflection for the parent phase recovered the former value (2.0 min). This value becomes always constant after annealing at any cycle. The desired setting temperature is always reached from 265 K with a cooling rate of 1 K/min. 265 K is higher than the inverse transition temperature. We have selected some fixed temperatures of 251.0 K–255.0 K, 255.25, 256.0, and 256.7 K to measure incubation time. As soon as temperature reached one of fixed temperatures, incubation time is counted. A precise temperature controller prevented any overshoot. The stability of temperature controller was better than ±0.05 K/h, ±0.1 K per day at a fixed temperature.

Figure 1(a) shows a typical time-dependent change of x-ray-diffraction patterns using the Si monochromator at 256.7 K. Figure 1(b) shows the same patterns at the same temperature using a HOPG monochromator. It is clear that the intensity of $(202)_{fct}$ Bragg peaks from variant I and variant II of the low-temperature phase gradually increases from t_s, phase transition start time while that of the $(220)_{fcc}$ Bragg peak of the parent phase decreases at the same time.

Figure 2 shows an example of the time-dependent diffraction patterns at 253 K using the HOPG monochromator. There is a significant difference between the time-dependent changes shown in Fig. 1 and that shown in Fig. 2. It was found that between 255 and 258 K, the intensity of two diffraction peaks corresponding to two variants of martensite phase as shown in Figs. 1(a) and 1(b) was steadily increasing with the lapse of time. On the other hand, between 250 and 225 K, more than two diffraction peaks appeared and their intensity changed eventually with the lapse of time. While in the former temperature range, the dependence of the x-ray-

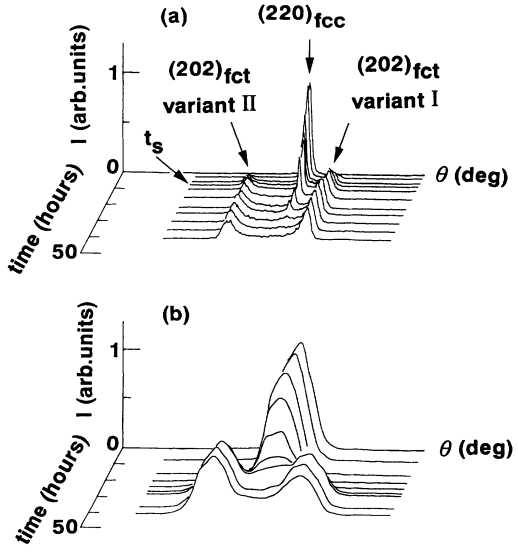

FIG. 1. Time dependence of diffraction pattern above T_p at 256.7 K with using (a) Si (311) and (b) HOPG (002) as monochromator. t_s corresponds to phase transition start time. $(220)_{fcc}$ Bragg reflection for the parent phase and $(202)_{fct}$ Bragg reflections from variant I and variant II for the low-temperature phase are pointed out at the peaks.

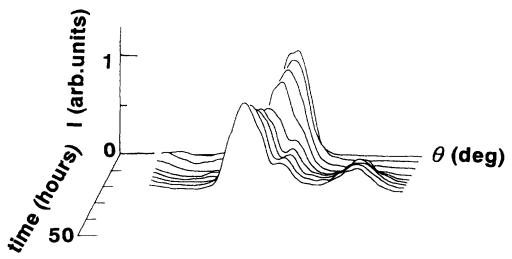

FIG. 2. Time dependence of diffraction patterns below T_p at 253 K with using HOPG (002) as monochromator.

diffraction pattern was quite reproducible, that in the latter temperature range was not reproducible.

In order to describe these experimental results, we introduce a new definition of T_p from the time dependence of diffraction patterns: above T_p, the diffraction pattern always shows the same reproducible time change and only two variants of the low-temperature phase appear, while below T_p, it shows a complicated time change due to appearance of many variants of the low-temperature phase. T_p in In 23 at. % Tl alloy is 255 K. The M_s of this sample is 250 K and T_0 is 258 K.

The incubation time, which was defined as waiting time until the phase transition starts at a fixed temperature, was about 10–50 h above T_p. The incubation time was measured just after the temperature reached at setting temperature. The fractional volume of the low-temperature phase, $X(t)$, is given by

$$X(t)=\frac{I(t)-I(0)}{I(\infty)-I(0)}\ , \tag{1}$$

where $I(t)$ is the integrated intensity of the $(202)_{\rm fct}$ Bragg reflection at the time t. $X(t)$ for various temperatures is shown in Fig. 3(a). A universal growth curve was obtained in the Cu_3Au system by plotting the growth curves at different temperatures against the scaled time $t/t_{1/2}$, where $t_{1/2}$ is defined by $X(t_{1/2})=\frac{1}{2}$. The growth curves in Fig. 3(a) were replotted using $t/t_{1/2}$, in Fig. 3(b). However, a universal growth curve, was not obtained in the present experiments. In the Cu_3Au system,[3] the growth curve was dominated by the increase of the domain size $L(t)$ according to the power law,

$$L(t)\propto t^{a}\ , \tag{2}$$

where a was constant. This suggested that the growth curves in the In-Tl alloy system were not controlled by the increase of the domain size. This is supported by the present experimental results that the FWHM of the low-temperature phase does not depend on time.

The $(202)_{\rm fct}$ Bragg reflections for the low-temperature phase started to increase at t_s as shown in Fig. 3(a), while the $(220)_{\rm fct}$ Bragg reflection for the parent phase started to decrease at the same time. Incubation time was characterized by $t_{1/2}$ rather than t_s, since it is difficult to define unambiguously the starting time t_s, due to the different initial slope of the growth curve at each temperature shown in Fig. 3 (b). The temperature dependence of the $t_{1/2}$-incubation time curves both of x-ray- and

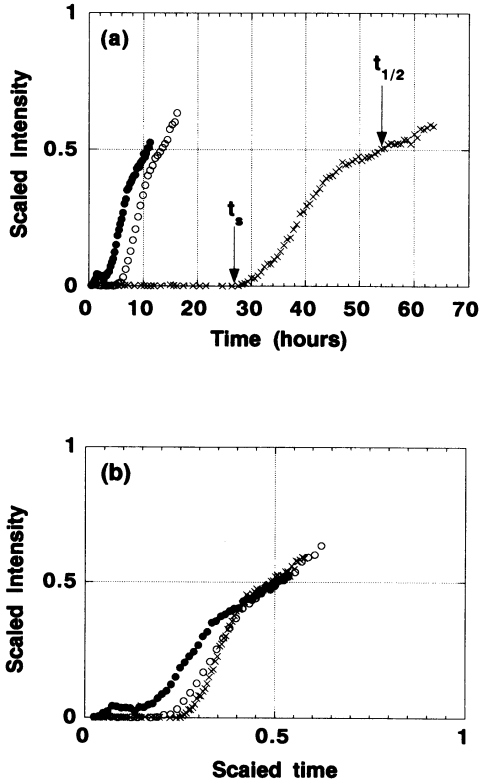

FIG. 3. Growth curves of low-temperature phase (a) scaled by intensity and (b) scaled by both intensity and $t_{1/2}$, $t_{1/2}$ is time when scaled intensity becomes $\frac{1}{2}$. t_s corresponds to phase transition start time. ●; 255.25 K, ○; 256.0 K, and ×; 256.7 K.

neutron-diffraction experiments is shown in Fig. 4. Moreover, $t_{1/2}$ becomes longer when T is close to T_0.

The relationship between the temperature and the $t_{1/2}$-incubation time is analyzed in terms of the nucleation process which is a thermal activation process described by the Boltzmann factor. The nucleation probability p and the incubation time t is assumed to depend only on the nucleation barrier. Hence,

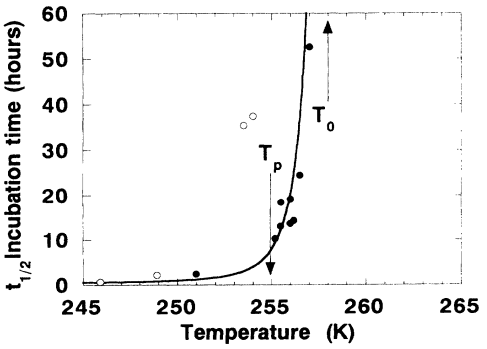

FIG. 4. $t_{1/2}$-incubation time vs temperature. Solid line shows calculated incubation time. T_p is peculiar temperature derived from the different growth process. T_0 is defined by $\Delta G(T_0)=0$; $\Delta G(T)$ is the difference of free energy between parent phase and low-temperature phase. ●; x-ray and ○; neutron.

$$p \propto \exp\left[-\frac{\Delta}{k_B T}\right], \quad t \propto \frac{1}{p}, \tag{3}$$

where p is nucleation probability, Δ is the nucleation barrier, k_B is Boltzmann's constant. Here, we have calculated the nucleation barrier using the Roitburd method.[8] The nucleation barrier diverges when temperature comes up to T_0. Figure 5 shows two kinds of curves. One set of curves is nucleation barrier (a) and nucleation probability (b) against temperature calculated assuming single-domain martensite (considered valid for $T < M_s$). The other set of curves is calculated by the same method but assuming multiple-domain martensite with the width of domain ~510 nm (considered valid for $T > M_s$). The new definition of T_p is quite different from M_s, martensite start temperature. Only two variants of twinned structure was obtained not only from the x-ray experiment but also from the bulk neutron experiment above T_p. On the other hand, below T_p, the low-temperature phase had a complicated time development of diffraction patterns and many Bragg reflections of the low-temperature phase appeared from various variants. Next we calculated nucleation probability and incubation time by using Eq. (3) and the nucleation barrier derived from the Roitburd method [Fig. 5(b)]. The nucleation probability becomes zero when the temperature is more than T_0. T_0 was determined as 258 K from the nucleation probability shown in Fig. 5(b) and inverse transition temperature, A_s(=261.8 K). Calculated incubation time is shown by the solid line in Fig. 4. Furthermore, incubation time of the neutron experiment was longer than that of the x-ray one. It is difficult to interpret the difference between the $t_{1/2}$'s value at the present time. However, we do not consider this due to the surface effect at least because of the following consideration. The scattering volume for neutron diffraction is larger than the corresponding quantity to x ray. Thus, it can be estimated that $t_{1/2}$ for the neutron-diffraction experiment is longer than that for the x-ray-diffraction experiment.

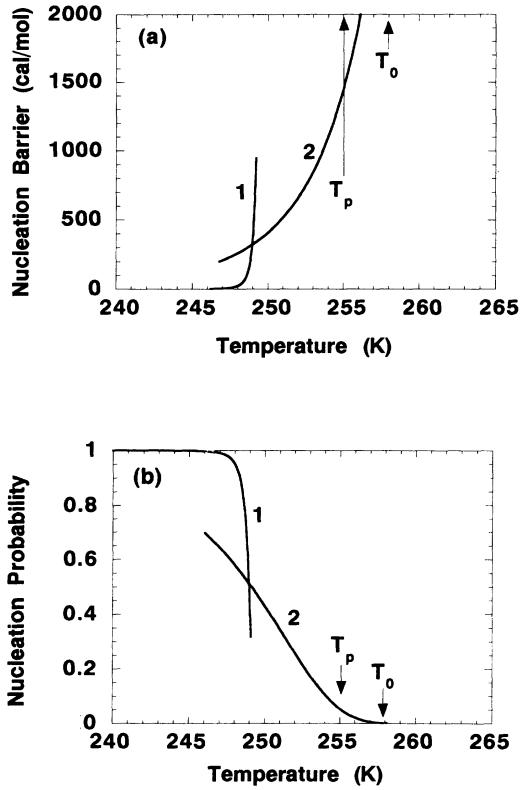

FIG. 5. (a) Calculated nucleation barrier by the Roitbund method and (b) nucleation probability derived from nucleation barrier: curve 1, single-domain (single-crystal) martensite; curve 2, multiple-domain (twinned) martensite. T_p is peculiar temperature derived from the different growth process. T_0 is defined by $\Delta G(T_0)=0$; $\Delta G(T)$ is the difference of free energy between parent phase and low-temperature phase.

IV. DISCUSSION

Incubation time should be an essential property of first-order phase transition. However, all of the first-order phase transitions do not always have incubation time, since incubation time will disappear if some dislocations or impurities provide a favorable site for nucleation. Incubation time is originated from the embryos of the low-temperature phase which is in the dynamic nonequilibrium state; its size is estimated to be about 1 nm ($T > T_p$) (Refs. 9 and 15) and its structure is not exactly identical to the low-temperature one. Once the size of the dynamic embryo is over a critical value, the nucleus becomes static and has the same structure at the low-temperature phase. We call these static nuclei "frozen nuclei."

The nucleation process as mentioned above is a universal phenomenon in the first-order phase transition. In contrast to this, the growth process depends on volume change from the parent phase to the low-temperature phase. The different behavior of metallic sodium and In-Tl alloys enable us to understand the relation between growth process and strain field. The phase transition of In-Tl alloys above T_p is regarded as an ideal nucleation and growth process, because between T_0 and T_p, the driving force, $\Delta G(T)$, is very small and the low-temperature phase, frozen nuclei, cannot grow extensively. Also in In-Tl alloys, volume change in phase transition is quite small. Since the strain field is not so long range even below M_s, the strain field has little influence on the growth process. Hence, the mutual interference among the frozen nuclei is negligible. Although metallic sodium is also found to show significant incubation time, the growth process of the low-temperature phase is entirely different from that in In-Tl alloys because of the large volume change and large strain field. An ideal nucleation and growth shown in In-Tl alloys between T_p and T_0 cannot be found in metallic sodium. It was observed that the FWHM was changed within a few minutes after incubation time.[11] The phase transition took place as a chain reaction by large strain.

ACKNOWLEDGMENTS

The authors would like to thank Professor T. Kakeshita of Osaka University and Professor Y. Matsuo of Nara

Women's University for helpful discussions. This study was supported by a Grant-in-Aid for Scientific Research (Nos. 02402045 and 05452271) and a Grant-in-Aid for Cooperative Research (No. 04302053) from the Ministry of Education, Science and Culture and Monbusho International Scientific Research Program (No. 04044032). Additional support was provided by the University of Tsukuba Project Research.

[1]Y. Noda, S. Nishihara, and Y. Yamada, J. Phys. Soc. Jpn. **53**, 4241 (1984).
[2]S. E. Nagler, R. F. Shannon, Jr., C. R. Harkless, and M. A. Singh, Phys. Rev. Lett. **61**, 718 (1988).
[3]R. F. Shannon, Jr., S. E. Nagler, C. R. Harkless, and R. M. Nicklow, Phys. Rev. B **46**, 40 (1992).
[4]N. Hamaya, Y. Yamada, J. D. Axe, D. P. Belanger, and S. M. Shapiro, Phys. Rev. B **33**, 7770 (1986).
[5]G. B. Olson and M. Cohen, Metall. Trans. A **7**, 1905 (1976).
[6]G. B. Olson and M. Cohen, Acta Metall. **27**, 1907 (1979).
[7]G. B. Olson, Acta Metall. **29**, 1475 (1981).
[8]A. L. Roitburd, Mater. Sci. Eng. A **127**, 229 (1990).
[9]T. Kakeshita, K. Kuroiwa, K. Shimizu, T. Ikeda, A. Yamagoshi, and M. Date, Mater. Trans. JIM **34**, 415 (1993).
[10]T. Kakeshita, K. Kuroiwa, K. Shimizu, T. Ikeda, A. Yamagoshi, and M. Date, Mater. Trans. JIM **34**, 423 (1993).
[11]H. Abe, K. Ohshima, T. Suzuki, S. Hoshino, and K. Kakurai, Phys. Rev. B **49**, 3739 (1994).
[12]N. Toyoshima, K. Harada, H. Abe, K. Ohshima, T. Suzuki, M. Wuttig, and T. R. Finlayson, J. Phys. Soc. Jpn. **63**, 1808 (1994).
[13]T. R. Finlayson and H. G. Smith, Metall. Trans. A **19**, 193 (1988).
[14]S. M. Shapiro and S. C. Moss, Phys. Rev. B **15**, 2726 (1977).
[15]T. Suzuki, Metall. Trans. A **12**, 709 (1981).